



ISSN: 0067-2904

Analyze a Temperature and MHD Peristaltic Flow of Jeffrey Fluid through a Porous Wavechannel in a Rotating Frame

Dheia G. Salih Al-Khafajy *, Anaam Mahdi Abbas Al-Kelabiy

Department of Mathematics, College of science, University of Al-Qadisiyah, Diwaniya, Iraq

Received: 11/2/2023

Accepted: 11/6/2023

Published: 30/6/2024

Abstract

The aim of this paper is to analyse the temperature and magnetohydrodynamic (MHD) peristaltic flow of Jeffrey fluid through a porous wave channel under the influence of rotation. The study is in Cartesian coordinates, the system of equations governing this issue is nonlinear and non-homogeneous partial differential. For the purpose of solving this system, we assumed a short wavelength and a very low Reynolds number due to the flow channel structure. After obtaining the system solution, we used the Mathematica 13 program to analyse the results through graphs. It observed that the rotation, magnetic field, viscosity and density of the fluid have an effective effect on the fluid movement and its temperature.

Keywords: Wave channel, Rotation, Magnetohydrodynamic (MHD), Cartesian coordinates, Jeffrey Fluid.

تحليل درجة الحرارة و التدفق التمعجي الهيدروديناميكي الممغنط لمائع جيفري خلال قناة موجية مسامية بإطار دوار

ضياء غازي صالح*, انعام مهدي عباس

قسم الرياضيات، كلية العلوم، جامعة القادسية، الديوانية، العراق

الخلاصة

الهدف من هذا البحث هو تحليل درجة الحرارة والتدفق التمعجي الهيدروديناميكي الممغنط لمائع جيفري عبر قناة موجية مسامية تحت تأثير الدوران. الدراسة بالإحداثيات الديكارتيّة، ونظام المعادلات التي تحكم هذه المسألة هي "تفاضلية جزئية غير خطية وغير متجانسة". لغرض حل هذا النظام، افترضنا طول موجي قصير ورقم رينولدز منخفض جداً (بسبب بنية قناة التدفق). بعد الحصول على حل النظام، استخدمنا برنامج Mathematica 13 لتحليل النتائج من خلال الرسوم البيانية. لوحظ أن الدوران والمجال المغناطيسي ومسامية قناة التدفق بالإضافة إلى لزوجة المائع وكثافته لها تأثير فعال على حركة المائع ودرجة حرارته.

1. Introduction

Peristaltic flow is a mechanism of fluid movement through a flow channel that arises from the flattening and contraction of the channel wall. Latham, the first author [1] whose work was on fluid motions in the peristaltic pump, and was followed by Shapiro et al. [2] where he presented a paper entitled peristaltic pumping at low long wavelengths. Furthermore, interest in magnetic-hydrodynamic peristaltic flow (MHD) has appeared for its many uses where

*Email: dr.dheia.g.salih@gmail.com

magnetic devices and magnetic particles are utilized as drug transferors, magnetic resonance imaging. MHD concepts are used in the strategy, design, and layout of pumps, heat exchangers, radar systems, power generators, flow meters, and other devices. In view of such physiological and industrial applications, MHD peristaltic flow has been studied with great interest by various researchers. Then a group of researchers followed them in analysing the magnetized hydrodynamic peristaltic flow of Jeffrey's fluid, see [3-7]. Jeffrey's fluid is an important non-Newtonian fluid because of its many applications in various fields (industrial or medical), see [4], and [6], so it was necessary to choose it as a model for a non-Newtonian fluid in our study. In the past few years, interest has begun to study the effect of rotation on the peristaltic flow of fluids, as Abd-Alla et al. [8] investigated the effect of rotation on the peristaltic flow of a micropolar fluid through a porous medium with an external magnetic field, see also [9]. Al-Aridhee and Al-Khafaj [10] investigated the influence of MHD peristaltic transport for the Jeffrey fluid with varying temperature and concentration through the porous medium. Later, Abdulhadi and Al-Hadad [11] study the effects of rotation and MHD on the nonlinear peristaltic flow of the Jeffery fluid in an asymmetric channel through a porous medium. Then Almusawi and Abdulhadi [12] introduced a model to analyse the heat transfer and magnetohydrodynamics effect on the peristaltic transport of Ree–Eyring fluid in a rotating frame. Recently, Hatem and Abdulhadi [13] and [14] investigated the effect of rotation on mixed convection heat transfer for the peristaltic transport of Bingham plastic fluid and viscoplastic fluid in an asymmetric channel.

Our goal is to present a mathematical model to analyse the temperature and hydrodynamic peristaltic flow of a Jeffrey fluid through a porous wave channel under the effect of rotation. This model simulates the movement of blood flow within the arteries and veins of the human body. Magnetic parameter is especially important stopping bleeding during surgical operations and its effect on lowering blood pressure inside the human body. Use graphs to discuss the velocity distribution, pressure distribution, friction forces, temperature profile, and trapping phenomenon.

2. Mathematical Formulation

Consider a peristaltic flow of Jeffrey fluid through a porous wave channel in two-dimensional Cartesian coordinates. The fluid is electrically conducted by an external magnetic field, $B = (0, B_0, 0)$. The fluid rotates with a uniform angular velocity Ω about the z-axis. Due to the wave motion of the flow channel wall (contraction and relaxation), the fluid moves in the form of a peristaltic flow in the middle of the channel. Note that the equation for the flow channel wall is $y = \pm W = \pm(d_1 - \bar{\phi} \sin^2((\bar{X} - s\bar{t})\pi/\omega))$, where the positive sign represents the upper wall while the negative sign represents the lower wall of the channel, and d_1 represents the tube's average radius, $\bar{\phi}$ is the peristaltic wave amplitude, \bar{t} is the time, ω is the wavelength, and s is the wave propagation speed.

The governed equations, continuity, momentum, and energy in two dimensions for incompressible, irrotational, laminar flow which in frame (\bar{X}, \bar{Y}) are expressed as:

$$\frac{\partial \bar{U}_1}{\partial \bar{X}} + \frac{\partial \bar{U}_2}{\partial \bar{Y}} = 0, \quad (1)$$

$$\rho \left(\frac{\partial \bar{U}_1}{\partial \bar{t}} + \bar{U}_1 \frac{\partial \bar{U}_1}{\partial \bar{X}} + \bar{U}_2 \frac{\partial \bar{U}_1}{\partial \bar{Y}} \right) - \Omega \rho \left(\Omega \bar{U}_1 + 2 \frac{\partial \bar{U}_2}{\partial \bar{t}} \right) = - \frac{\partial \bar{P}}{\partial \bar{X}} + \frac{\partial \bar{S}_{\bar{X}\bar{X}}}{\partial \bar{X}} + \frac{\partial \bar{S}_{\bar{X}\bar{Y}}}{\partial \bar{Y}} - \sigma B_0^2 \bar{U}_1 - \frac{\mu}{R} \bar{U}_1, \quad (2)$$

$$\rho \left(\frac{\partial \bar{U}_2}{\partial \bar{t}} + \bar{U}_1 \frac{\partial \bar{U}_2}{\partial \bar{X}} + \bar{U}_2 \frac{\partial \bar{U}_2}{\partial \bar{Y}} \right) - \Omega \rho \left(\Omega \bar{U}_2 - 2 \frac{\partial \bar{U}_1}{\partial \bar{t}} \right) = - \frac{\partial \bar{P}}{\partial \bar{Y}} + \frac{\partial \bar{S}_{\bar{Y}\bar{X}}}{\partial \bar{X}} + \frac{\partial \bar{S}_{\bar{Y}\bar{Y}}}{\partial \bar{Y}} - \frac{\mu}{R} \bar{U}_2, \quad (3)$$

$$\rho c_p \left(\frac{\partial}{\partial \bar{t}} + \bar{U}_1 \left(\frac{\partial}{\partial \bar{X}} \right) + \bar{U}_2 \left(\frac{\partial}{\partial \bar{Y}} \right) \right) T = H \left(\frac{\partial^2 T}{\partial \bar{x}^2} + \frac{\partial^2 T}{\partial \bar{y}^2} \right) + \frac{\partial \bar{U}_1}{\partial \bar{X}} (\bar{S}_{\bar{X}\bar{X}}) + \frac{\partial \bar{U}_1}{\partial \bar{X}} (\bar{S}_{\bar{X}\bar{Y}}) + \frac{\partial \bar{U}_2}{\partial \bar{Y}} (\bar{S}_{\bar{Y}\bar{X}}) + \frac{\partial \bar{U}_2}{\partial \bar{Y}} (\bar{S}_{\bar{Y}\bar{Y}}) - G(T - T_0). \quad (4)$$

Where Ω , B_0 , σ , \hat{K} , c_p , G , H and ρ refer to rotation parameter, magnetic field, electric conductivity, permeability, specific heat, heat source, thermal conductivity, and density of fluid, respectively.

The following relations are for converting from the test frame (\bar{X}, \bar{Y}) to the wave frame (\bar{x}, \bar{y}) :
 $(\bar{x}, \bar{y}) = (\bar{X} - s\bar{t}, \bar{Y})$, $\bar{U}_1 = \bar{u}_1 + s$, $\bar{U}_2 = \bar{u}_2$ and $\bar{P} = \bar{p}(\bar{x}, \bar{y})$. (5)

Where (\bar{u}_1, \bar{u}_2) and (\bar{U}_1, \bar{U}_2) are velocity components, and \bar{p} is the pressure in a wave.

3. Method of Solution

To simplify resolving the motion control equations, we present dimensionless equations

$$\left. \begin{aligned} x = \frac{\bar{x}}{\omega}, y = \frac{\bar{y}}{d_1}, \delta = \frac{d_1}{\omega}, u_1 = \frac{\bar{u}_1}{s}, u_2 = \frac{\omega \bar{u}_2}{s d_1}, H_c = \frac{G d_1^2}{\mu c_p}, p = \frac{d_1^2 \bar{p}}{\mu \omega s}, D_a = \frac{\hat{K}}{d_1^2}, \Phi = \frac{\bar{\Phi}}{d_1}, P_r = \frac{\mu c_p}{H}, \\ M_e = \frac{d_1^2}{\mu} \sigma B_0^2, E_c = \frac{s^2}{c_p(T_1 - T_0)}, S_{xx} = \frac{\omega \bar{s}_{xx}}{\mu s}, S_{xy} = \frac{d_1 \bar{s}_{xy}}{\mu s}, S_{yy} = \frac{\omega \bar{s}_{yy}}{\mu s}, Re = \frac{\rho s d_1}{\mu}, \theta = \frac{T - T_0}{T_1 - T_0} \end{aligned} \right\} \quad (6)$$

Where D_a refer to Darcy number, Ψ refer to stream function, Re refer to Reynolds number, Φ amplitude ratio, δ refer to dimensionless wave number, θ refer to dimensionless temperature, M_e refer to magnetic parameter, H_c refer to heat source parameter, E_c refer to Eckert number, and P_r refer to Prandtl number.

Substituting Eqs. (5,6) into Eqs. (1-4) and after simplifying, we obtain:

$$\frac{\partial u_1}{\partial x} + \frac{\partial u_2}{\partial y} = 0, \quad (7)$$

$$\begin{aligned} R_e \delta \left((u_1 + 1) \frac{\partial u_1}{\partial x} + u_2 \frac{\partial u_1}{\partial y} \right) - \frac{\rho d_1^2}{\mu} \Omega^2 (u_1 + 1) = -\frac{\partial p}{\partial x} + \delta^2 \frac{\partial S_{xx}}{\partial x} + \frac{\partial S_{xy}}{\partial y} - \\ \left(M_e^2 + \frac{1}{D_a} \right) (u_1 + 1), \end{aligned} \quad (8)$$

$$R_e \delta^3 \left((u_1 + 1) \frac{\partial u_2}{\partial x} + u_2 \frac{\partial u_2}{\partial y} \right) - \delta^2 \frac{\rho d_1^2}{\mu} \Omega^2 u_2 = -\frac{\partial p}{\partial y} + \delta^2 \frac{\partial S_{yx}}{\partial x} + \delta \frac{\partial S_{yy}}{\partial y} - \delta^2 \frac{1}{D_a} u_2, \quad (9)$$

$$\begin{aligned} R_e \delta \left((u_1 + 1) \frac{\partial \theta}{\partial x} + u_2 \frac{\partial \theta}{\partial y} \right) = \frac{1}{P_r} \left(\delta^2 \frac{\partial^2 \theta}{\partial x^2} + \frac{\partial^2 \theta}{\partial y^2} \right) + E_c \left(\delta^2 \frac{\partial u_1}{\partial x} (S_{xx}) + \delta^2 \frac{\partial u_2}{\partial x} (S_{xy}) + \right. \\ \left. \frac{\partial u_1}{\partial y} (S_{yx}) + \delta^2 \frac{\partial u_2}{\partial y} (S_{yy}) \right) - H_c \theta. \end{aligned} \quad (10)$$

The dimensionless extra stress tensor components of Jeffrey's fluid takes on the following form:

$$S_{xx} = \frac{2}{1+\lambda_1} \left(\frac{\partial u_1}{\partial x} \right), S_{yy} = \frac{2}{1+\lambda_1} \left(\frac{\partial u_2}{\partial y} \right), \text{ and } S_{xy} = \frac{1}{1+\lambda_1} \left(\frac{\partial u_1}{\partial y} \right) \quad (11)$$

Where λ_1 , and μ are the ratio between relaxation to retardation times, and viscosity fluid, respectively.

The associated dimensionless boundary conditions in the wave frame are:

$$u_1 = -1 \text{ at } y = \pm w = \pm(1 - \Phi \sin^2(\pi x)), \quad (12)$$

$$\theta = 0 \text{ at } y = w = -1 + \Phi \sin^2(\pi x), \text{ and } \theta = 1 \text{ at } y = -w = 1 - \Phi \sin^2(\pi x). \quad (13)$$

The structure of the flow channel assumed the wavelength δ is very small ($\ll 1$), and therefore after simplification and neglecting the parts in which this parameter appears in Eqs. (8-10), we obtain

$$-\frac{\rho d_1^2}{\mu} \Omega^2 (u_1 + 1) = -\frac{\partial p}{\partial x} + \frac{\partial}{\partial y} S_{xy} - \left(M_e^2 + \frac{1}{D_a} \right) (u_1 + 1) \quad (14)$$

$$\frac{\partial p}{\partial y} = 0 \quad (15)$$

$$\frac{1}{P_r} \frac{\partial^2 \theta}{\partial y^2} + E_c S_{yx} \left(\frac{\partial u_1}{\partial y} \right) - H_c \theta = 0. \quad (16)$$

3.1 Velocity Function

Equation (15) shows that pressure depends on x only. Substituting extra stress S_{xy} from Eq.(11) into Eq. (14), we obtain

$$\frac{\partial^2 u_1}{\partial y^2} + (1 + \lambda_1) \left(\frac{\rho d_1^2}{\mu} \Omega^2 - \left(M_e^2 + \frac{1}{D_a} \right) \right) u_1 = (1 + \lambda_1) \left(\frac{dp}{dx} + \left(M_e^2 + \frac{1}{D_a} \right) - \frac{\rho d_1^2}{\mu} \Omega^2 \right). \quad (17)$$

The exact solution of the momentum Eq. (17) that satisfy the boundary conditions (12) is

$$u_1 = - \left(\frac{\left(\frac{dp}{dx} \right) \sec \left(w \sqrt{(1 + \lambda_1) \left(\frac{\rho d_1^2}{\mu} \Omega^2 - \left(M_e^2 + \frac{1}{D_a} \right) \right)} \right)}{\left(\frac{\rho d_1^2}{\mu} \Omega^2 - \left(M_e^2 + \frac{1}{D_a} \right) \right)} \right) \cos \left(y \sqrt{(1 + \lambda_1) \left(\frac{\rho d_1^2}{\mu} \Omega^2 - \left(M_e^2 + \frac{1}{D_a} \right) \right)} \right) + \frac{\left(\frac{dp}{dx} \right)}{\left(\frac{\rho d_1^2}{\mu} \Omega^2 - \left(M_e^2 + \frac{1}{D_a} \right) \right)} - 1 \quad (18)$$

$$\text{Where } \frac{dp}{dx} = \frac{\left(\frac{\rho d_1^2}{\mu} \Omega^2 - \left(M_e^2 + \frac{1}{D_a} \right) \right) (-2 + 2q + 4w + \phi) \sqrt{(1 + \lambda_1)}}{4 \left(w \sqrt{M_e^2 + \frac{1}{D_a} (1 + \lambda_1)} - \tan \left(w \sqrt{M_e^2 + \frac{1}{D_a} (1 + \lambda_1)} \right) \right)}. \quad (19)$$

We define the pressure rise Δp_ω and friction forces F_ω on the upper, and lower walls as

$$\Delta p_\omega = \int_0^1 \left(\frac{dp}{dx} \right) dx, \quad (20)$$

$$F_\omega = \int_0^1 (w)^2 \left(- \frac{dp}{dx} \right) dx. \quad (21)$$

We get very long solutions for the two equations (20) and (21) by the boundary conditions from Eq.(12), we will confine ourselves to interpreting the results graphically. Where $\frac{dp}{dx}$ from Eq. (19).

3.2 Temperature Function

To solve the temperature equation, we substitute velocity function u_1 and extra stress S_{xy} into Eq. (16), and we obtain

$$\frac{\partial^2 \theta}{\partial y^2} - P_r H_c \theta = - \frac{P_r E_c}{(1 + \lambda_1)} \left(\frac{\partial u_1}{\partial y} \right)^2. \quad (22)$$

The solution to the heat equation is rather long, we will discuss and analyze the solution through the heat function diagrams.

3.3 Stream Function

The corresponding stream function is $u_1 = \frac{\partial \Psi}{\partial y}$ so that

$$\Psi = \left(\frac{\left(\frac{dp}{dx} + (M_e^2 + \frac{1}{Da}) - \frac{\rho d_1^2 \Omega^2}{\mu} \right) y}{\left(\frac{\rho d_1^2 \Omega^2}{\mu} - (M_e^2 + \frac{1}{Da}) \right)} \right) \left(\begin{matrix} \text{Sec} \left(\sqrt{(1+\lambda_1) \left(\frac{\rho d_1^2 \Omega^2}{\mu} - (M_e^2 + \frac{1}{Da}) \right)} w \right) \\ \text{Sin} \left(\sqrt{(1+\lambda_1) \left(\frac{\rho d_1^2 \Omega^2}{\mu} - (M_e^2 + \frac{1}{Da}) \right)} y \right) \end{matrix} \right) \left(\frac{\left((1+\lambda_1) \left(\frac{\rho d_1^2 \Omega^2}{\mu} - (M_e^2 + \frac{1}{Da}) \right) + (1+\lambda_1) \left(\frac{dp}{dx} + (M_e^2 + \frac{1}{Da}) - \frac{\rho d_1^2 \Omega^2}{\mu} \right) \right)}{(1+\lambda_1) \left(\frac{\rho d_1^2 \Omega^2}{\mu} - (M_e^2 + \frac{1}{Da}) \right)^{\frac{3}{2}}} \right) \tag{23}$$

Where $\frac{dp}{dx}$ from Eq. (19).

4. Discussion of the Results

In this section, we discuss and analyze the temperature and MHD peristaltic flow of Jeffrey fluid through a porous wave channel under the influence of rotation by using the "Mathematica 13" program. This section is divided into six subsections: the first covers the impact of parameters on fluid movement, the second discusses the impact of parameters on pressure gradient, the third and fourth analyse the impact of parameters on pressure rise and friction forces, respectively. Fifth analyse the impact of parameters on temperature, and the final subsection analyses the impact of parameters on stream function.

4.1 Velocity Distribution

Figure (1) from (1a-1d) show that the effect of parameters $q1$, Ω , ϕ , Da , ρ , d_1 , λ_1 and M_e , respectively, on the distribution of velocity. Figures (1a) and (1b) show the velocity u_1 increase with increase the parameters $q1$, Ω , ϕ , and Da . The velocity increases in the middle of the channel and decreases near the channel's walls due to the increase of the two parameters ρ and d_1 as shown in figure (1c). Figure (1d), we see that the velocity u_1 decreases in the middle of channel, the velocity u_1 increase near the channel's walls with an increase λ_1 , and M_e , respectively.

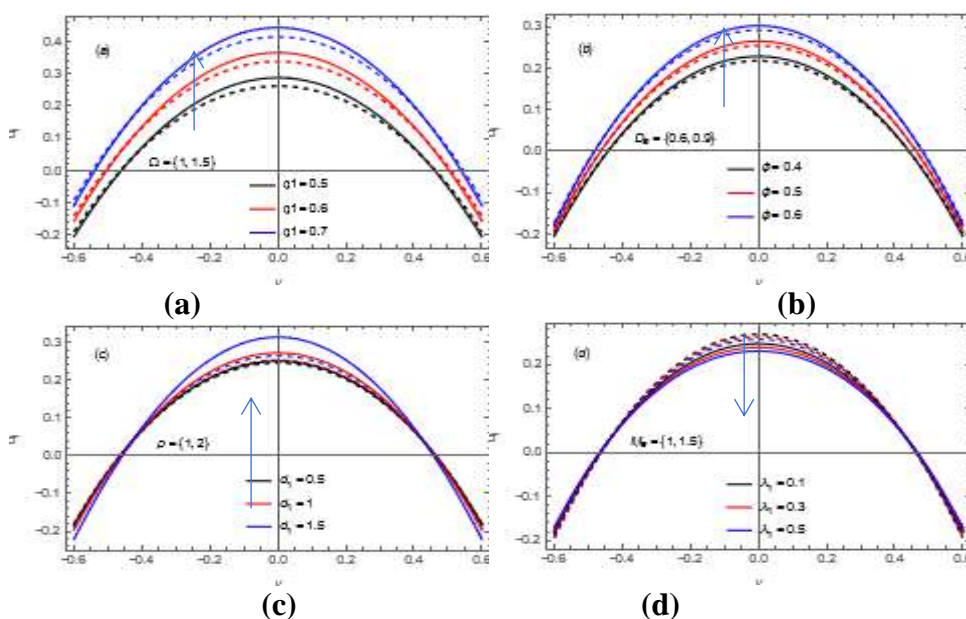


Figure 1: Variation of the velocity distribution for the following set of parameters $q1 = 0.5, \phi = 0.5, \Omega = 1, \rho = 2, Da = 0.8, d_1 = 1, \lambda_1 = 0.2, \mu = 2, M_e = 1.3, x = 0.1$.

4.2 Pressure Gradient

The influence of parameters $q_1, \mu, \lambda_1, M_e, \Omega, d_1, \rho,$ and D_a on the pressure gradient dp/dx are discussed. Figure (2a) shows that the pressure gradient increases with an increase in the parameters q_1 and μ . Figure (2b) shows that the pressure gradient increases with an increase λ_1 , and M_e . Figures (2c) and (2d) show that the pressure gradient decreases with an increase $\Omega, d_1, \rho,$ and D_a , respectively.

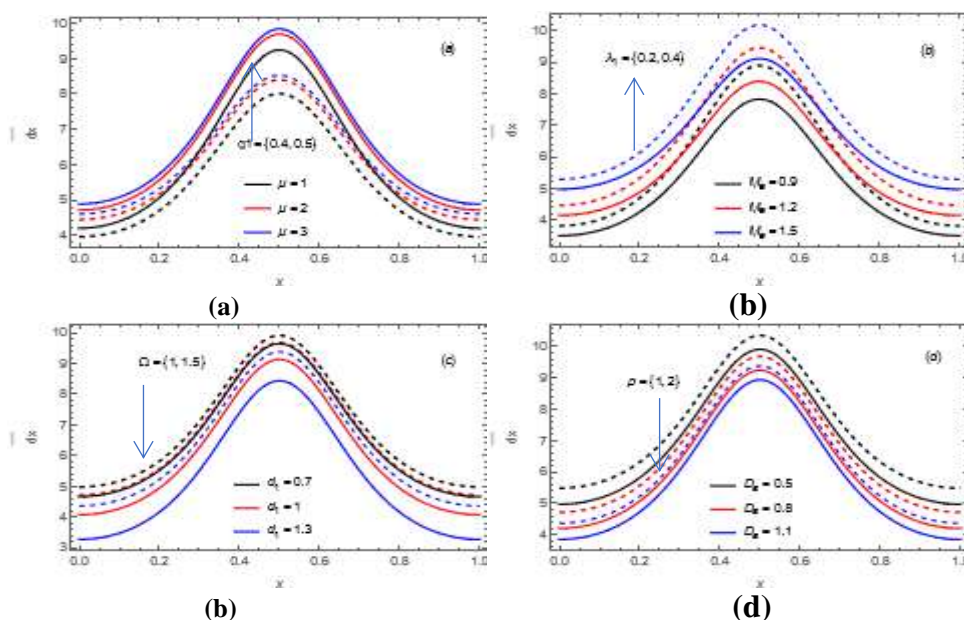


Figure 2: Variation of the pressure gradient for the following set of parameters: $q_1 = 0.5, \phi = 0.5, \Omega = 1, \rho = 2, D_a = 0.8, d_1 = 1, \lambda_1 = 0.2, \mu = 2, M_e = 1.3, x = 0.1$.

4.3 Pressure Rise

Figure (3a-3d) show the effects of the parameters $q_1, \mu, \lambda_1, M_e, \phi, D_a, \rho,$ and d_1 , respectively, on the pressure rise Δp_ω vs. Ω , through the region $-1 < \Omega < 1$. It is clear that the pressure rise take the form of a parabola towards the bottom, it take the highest value when $\Omega = 0$ and when the value of Ω moves away from zero, we notice that the curve decreases. In addition, we notice the value of Δp_ω increase or decrease according to the parameter. Notice that the pressure increase with an increase in the $q_1, \mu, \lambda_1, M_e, D_a,$ and ϕ , while Δp_ω decreases with an increase in $\rho,$ and d_1 , respectively.

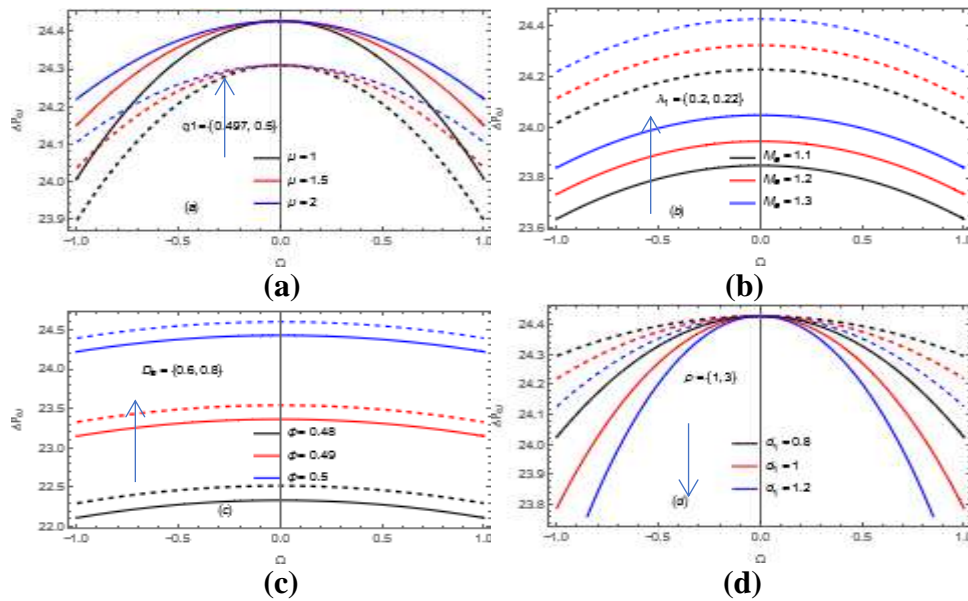


Figure -3: Variation of the pressure rise for the following set of parameters $q1 = 0.5, \phi = 0.5, \rho = 2, D_a = 0.8, d_1 = 1, \lambda_1 = 0.2, \mu = 2, M_e = 1.3, x = 0.1$.

4.4 Friction Forces

Figures from (4a-4d) are shown that the effect of the parameters $q1, \phi, \mu, M_e, D_a, \lambda_1, \rho,$ and d_1 on the friction forces F_ω vs. Ω . It is clear that the friction forces curve is in the form of a parabola towards the top and the lowest value when $\Omega = 0$, and when Ω moves away from zero, right or left, we notice that the curve is increasing. In addition, we note that the value of F_ω increases or decreases according to the parameters, as the friction forces increases with increasing ρ , and d_1 , while F_ω decreases with increasing $q1, \mu, M_e, \lambda_1, D_a$ and ϕ , respectively.

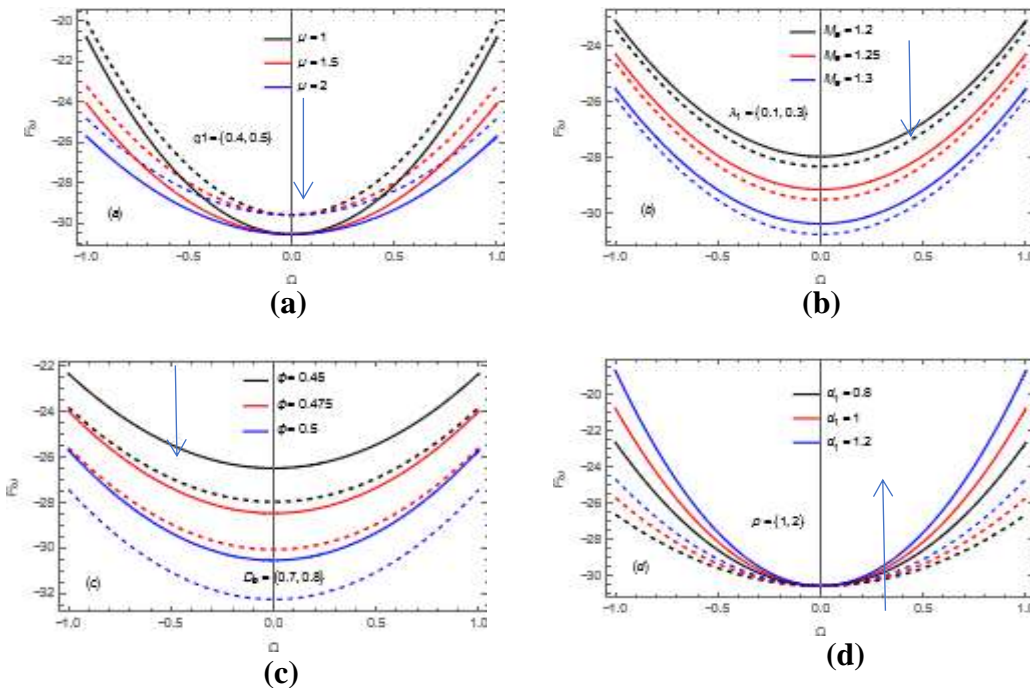


Figure 4: Variance of the friction forces for the following set of parameters $q1 = 0.5, \phi = 0.5, \rho = 2, D_a = 0.8, d_1 = 1, \lambda_1 = 0.2, \mu = 2, M_e = 1.3, x = 0.1$.

4.5 Temperature profile

Figures (5a-5f) are shown the effect of parameters $q_1, \lambda_1, Pr, \mu, \Omega, E_c, d_1, H_c, \phi, D_a, \rho,$ and M_e on the temperature vs. y . We note that the general form of the temperature distribution is curve proportional to the boundary conditions from Eq. (13). Furthermore, we notice the temperature of fluid increase with the increase of the parameters $\Omega, E_c, H_c, d_1, D_a$ and ϕ , while the temperature decreases with the increase of the parameters $q_1, \lambda_1, Pr, \mu, \rho,$ and M_e , respectively.

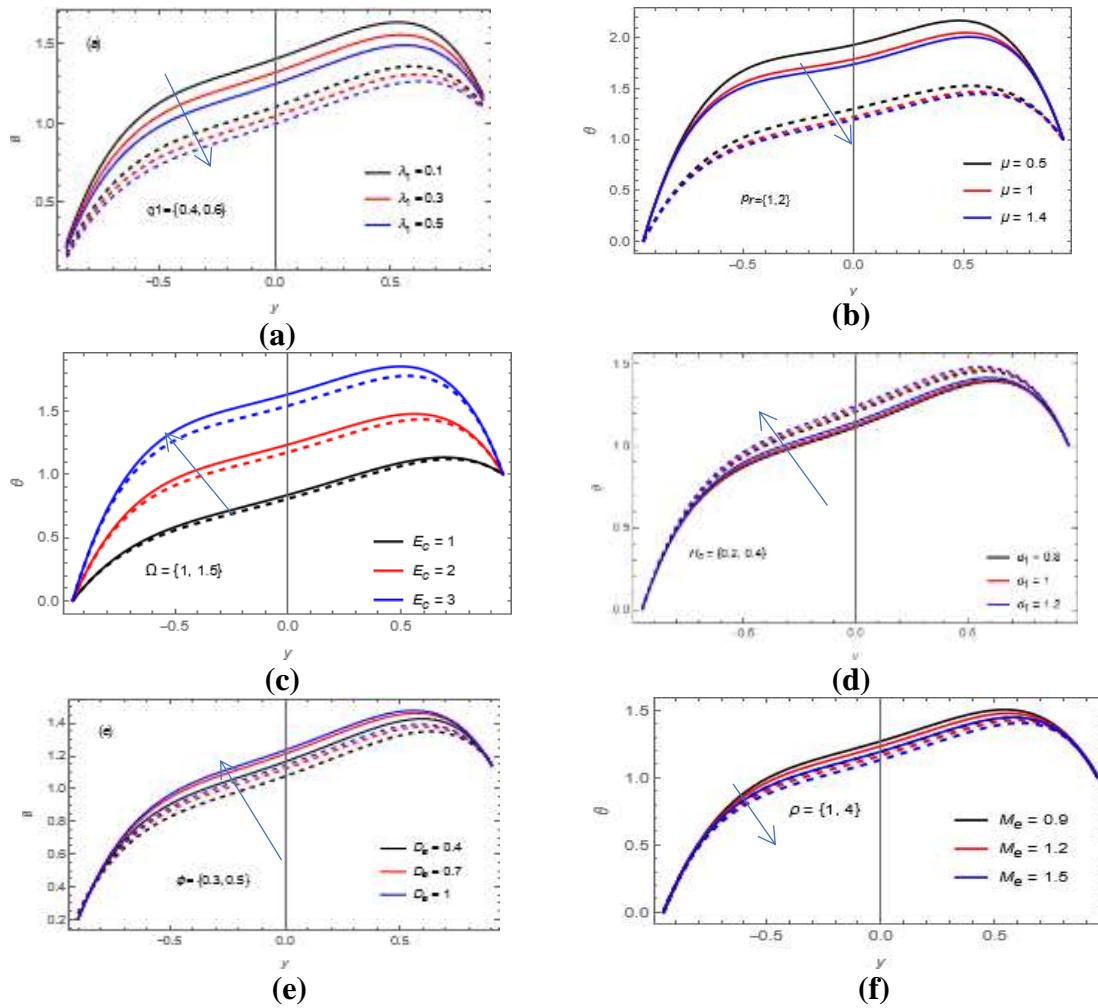


Figure 5: Variation of the temperature distribution for the following set of parameters $q_1 = 0.5, \lambda_1 = 0.2, \phi = 0.5, \rho = 2, d_1 = 1, \mu = 2, \Omega = 1, E_c = 2, H_c = 0.3, Pr = 1, M_e = 1.3, D_a = 0.8, x = 0.1$.

4.6 Trapping Phenomenon

The creation of fluid internal bolus by a closed streamline in a fluid flow is known as the trapping phenomenon. Subsection, we will explain the influence of the parameters $q_1, \lambda_1, \Omega, d_1, D_a, \phi, M_e$ and μ on trapped bolus through a porous wave channel. Figures (6a-6f) seen that the trapped bolus increases and grows steadily in the channel's center and expands to the outer walls by increasing parameters $q_1, \lambda_1, \Omega, d_1, D_a$ and ϕ , respectively, and vice versa when with respect to M_e , and μ , their effect are the contraction of the trapped bolus, see Figures (6.g,6.h).

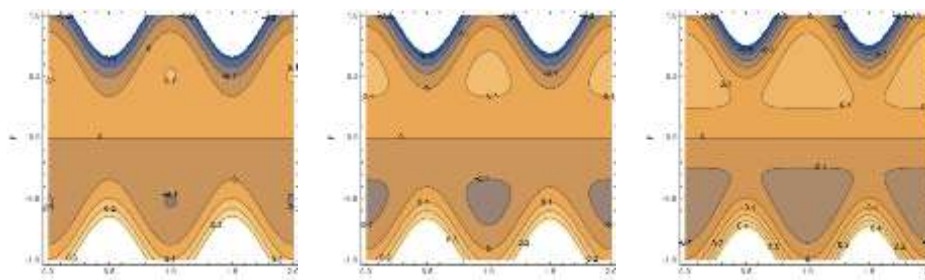


Figure 6a: Stream function of $q_1 = \{0.5401, 0.6, 0.73\}$ with $\phi = 0.5, \Omega = 1, \rho = 2, D_a = 0.8, d_1 = 1, \lambda_1 = 0.2, \mu = 2, M_e = 1.3, x = 0.1$.

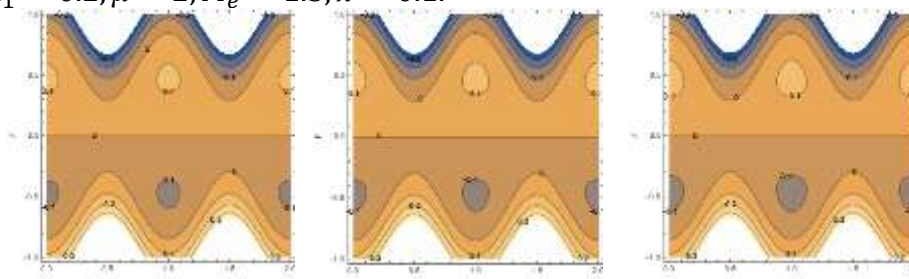


Figure 6b: Stream function of $\lambda_1 = \{0.1, 0.5, 1\}$ with $q_1 = 0.5, \phi = 0.5, \Omega = 1, \rho = 2, D_a = 0.8, d_1 = 1, \mu = 2, M_e = 1.3, x = 0.1$.

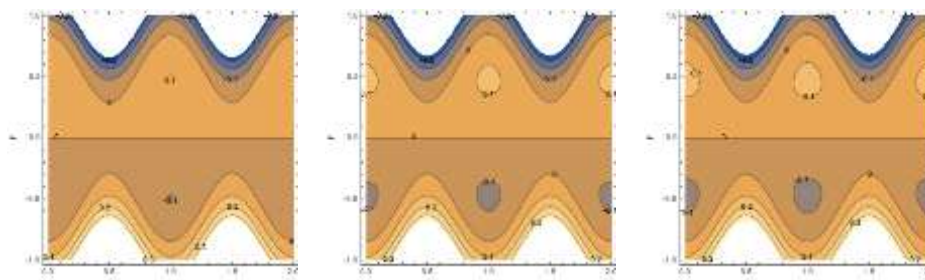


Figure 6c: Stream function of $\Omega = \{0.67, 2, 2.225\}$ with $q_1 = 0.5, \phi = 0.5, \rho = 2, D_a = 0.8, d_1 = 1, \lambda_1 = 0.2, \mu = 2, M_e = 1.3, x = 0.1$.

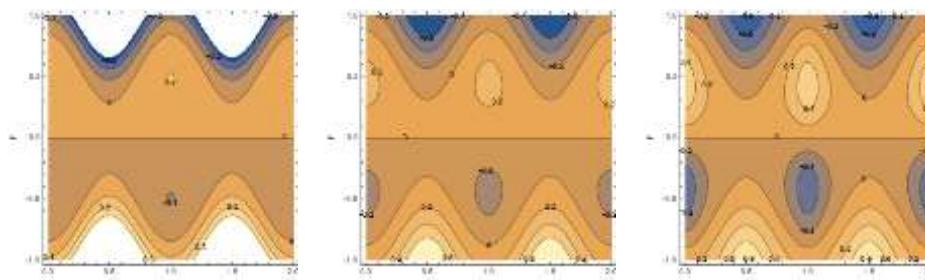


Figure 6d: Stream function of $d_1 = \{1.7, 3.5, 4\}$ with $q_1 = 0.5, \phi = 0.5, \Omega = 1, \rho = 2, D_a = 0.8, \lambda_1 = 0.2, \mu = 2, M_e = 1.3, x = 0.1$.

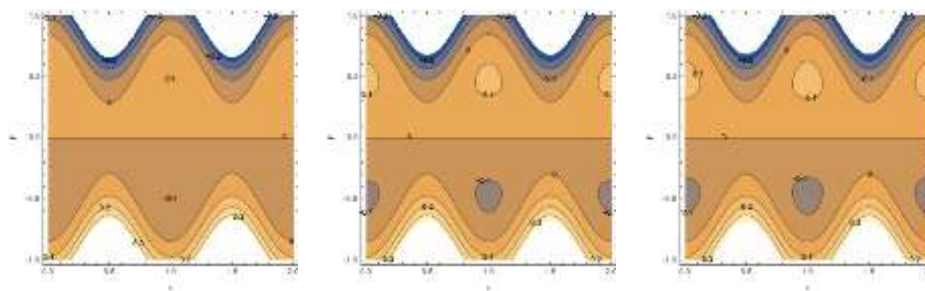


Figure 6e: Stream function of $D_a = \{0.4, 1, 2\}$ with $q_1 = 0.5, \phi = 0.5, \Omega = 1, \rho = 2, d_1 = 1, \lambda_1 = 0.2, \mu = 2, M_e = 1.3, x = 0.1$.

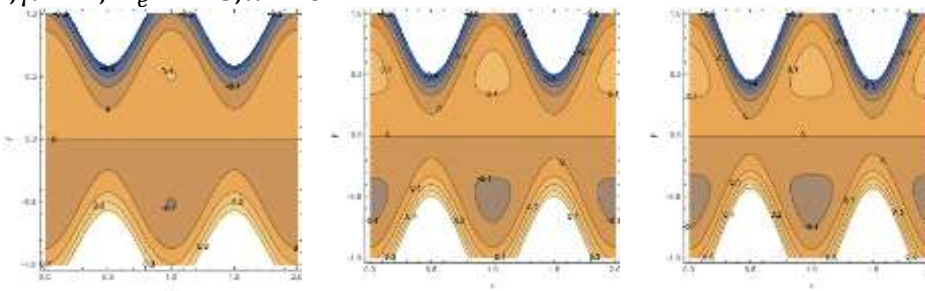


Figure 6f: Stream function of $\Phi = \{0.575, 0.69, 0.746\}$ with $q_1 = 0.5, \Omega = 1, \rho = 2, D_a = 0.8, d_1 = 1, \lambda_1 = 0.2, \mu = 2, M_e = 1.3, x = 0.1$.

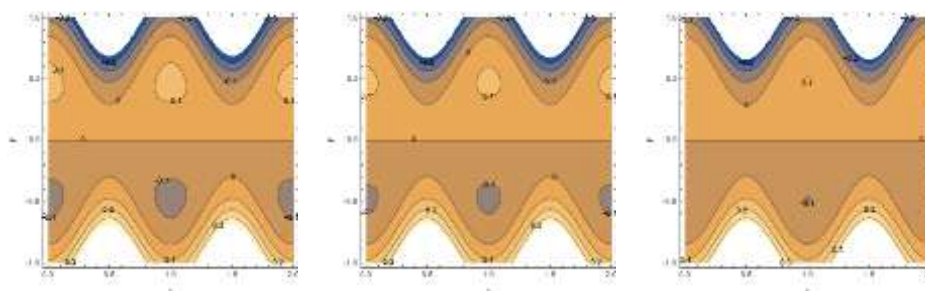


Figure 6g: Stream function of $M_e = \{0.8, 1, 2\}$ with $q_1 = 0.5, \phi = 0.5, \Omega = 1, \rho = 2, D_a = 0.8, d_1 = 1, \lambda_1 = 0.2, \mu = 2, x = 0.1$

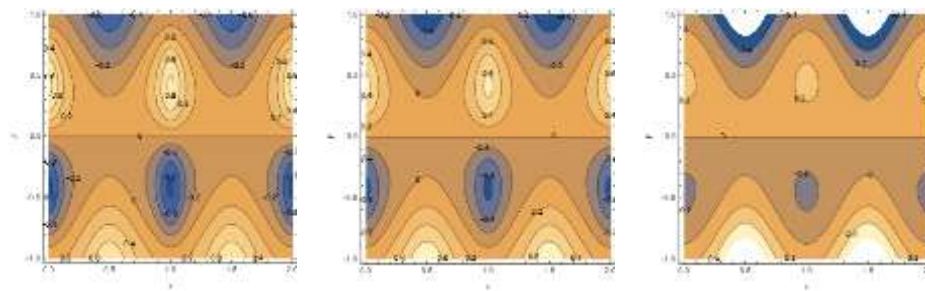


Figure 6h: Stream function of $\mu = \{0.115, 0.12, 0.17\}$ with $q_1 = 0.5, \phi = 0.5, \Omega = 1, \rho = 2, D_a = 0.8, d_1 = 1, \lambda_1 = 0.2, M_e = 1.3, x = 0.1$

5. Concluding Remarks

This study is concerned with analysing the effect of rotation in addition to several parameters on the temperature and hydrodynamic peristaltic flow of the Jeffrey fluid through a porous wave channel. Furthermore, the pressure gradient, the pressure rise, the distribution

of friction forces, and the flow function are studied. Below we include a summary of our study

- i. The fluid velocity and temperature increase with the increase of the parameters q_1 , Ω , ϕ , D_a , ρ , and d_1 , respectively, while the fluid velocity and temperature decrease with the increase of the parameters μ , λ_1 , and M_e . In addition, we notice that the fluid temperature rises with the increase in P_r , E_c , while its temperature decreases with the increase in the parameter H_c .
- ii. The pressure gradient increase with the increase in the parameters q_1 , μ , ρ and D_a , respectively, while the pressure gradient decrease with the increase in the parameters d_1 , Ω , M_e , and λ_1 .
- iii. the pressure increase with the increase in the parameters q_1 , μ , λ_1 , M_e , D_a and ϕ , while the pressure decreased with the increase in the parameters ρ , and d_1 . Conversely, a decrease in the value of friction force with the increase of the parameters q_1 , μ , λ_1 , M_e , D_a and ϕ , while friction force increases with the increase in the parameters ρ , and d_1 .
- iv. If the rotation increase, the pressure on the canal wall decreases. This is evident from the inverse relationship between the pressure gradient and the rotation parameter.
- v. The pressure rises at its highest value when the rotation is zero. The value decreases when the rotation parameter takes values far from zero negative or positive, the effect of rotation on the friction forces is a opposite, where the value of the friction forces is lowest when the rotation is zero, then Its value increases when the rotation parameter takes values far from zero (negative or positive).
- vi. The trapped bolus grows and expands to the outside wall as the parameters q_1 , λ_1 , Ω , d_1 , D_a and ϕ increase, while an increase in the value of M_e , and μ leads to narrowing it.

References

- [1] T. W. Latham, "Fluid motions in a peristaltic pump," *Massachusetts Institute of Technology*, 1966.
- [2] A. H. Shapiro, M. Y. Jaffrin, and S. L. Weinberg, "Peristaltic pumping with long wavelengths at low Reynolds number," *Journal of fluid mechanics*, vol. 37, no. 4, pp. 799-825, 1969.
- [3] A. Sinha, G. Shit, and N. Ranjit, "Peristaltic transport of MHD flow and heat transfer in an asymmetric channel," Effects of variable viscosity, velocity-slip and temperature jump," *Alexandria Engineering Journal*, vol. 54, no. 3, pp. 691-704, 2015.
- [4] D. G. S. Al-Khafajy, "Influence of Varying Temperature and Concentration on (MHD) Peristaltic Transport for Jeffrey Fluid through an Inclined Porous Channel," *Journal of Physics: Conference Series*, vol. 1664, no. 1: IOP Publishing, p. 012030, 2020.
- [5] D. G. S. Al-Khafajy, "Influence of Varying Temperature and Concentration on "Magnetohydrodynamics Peristaltic Transport for Jeffrey Fluid with a Nanoparticles Phenomenon through a Rectangular Porous Duct," *Baghdad Science Journal*, vol. 18, no. 2, 2021.
- [6] D. G. S. Al-Khafajy and A. Noor, "The Peristaltic Flow of Jeffrey Fluid through a Flexible Channel," *Iraqi Journal of Science*, pp. 5476-5486, 2022.
- [7] A. Abd-Alla, S. Abo-Dahab, and R. Al-Simery, "Effect of rotation on peristaltic flow of a micropolar fluid through a porous medium with an external magnetic field," *Journal of magnetism and Magnetic materials*, vol. 348, pp. 33-43, 2013.
- [8] A. Abd-Alla, S. Abo-Dahab, and H. El-Shahrany, "Effects of rotation and magnetic field on the nonlinear peristaltic flow of a second-order fluid in an asymmetric channel through a porous medium," *Chinese Physics B*, vol. 22, no. 7, p. 074702, 2013.
- [9] A. Abd-Alla and S. Abo-Dahab, "Rotation effect on peristaltic transport of a Jeffrey fluid in an asymmetric channel with gravity field," *Alexandria Engineering Journal*, vol. 55, no. 2, pp. 1725-1735, 2016.
- [10] A. A. Hussien. Al-Aridhee and Dheia G. S. Al-Khafajy, "Influence of MHD Peristaltic Transport for Jeffrey Fluid with Varying Temperature and Concentration through Porous Medium," *Journal of Physics: Conference Series*, vol. 1294, no. 3: IOP Publishing, p. 032012, 2019.

- [11] A. M. Abdulhadi and A. H. Al-Hadad, "Effects of rotation and MHD on the Nonlinear Peristaltic Flow of a Jeffery Fluid in an Asymmetric Channel through a Porous Medium," *Iraqi journal of science*, vol. 57, no. 1A, pp. 223-240, 2016.
- [12] B. A. Almusawi and A. M. Abdulhadi, "Heat Transfer Analysis and Magnetohydrodynamics Effect on Peristaltic Transport of Ree–Eyring Fluid in Rotating Frame," *Iraqi Journal of Science*, vol. 62, no. 8, pp. 2714-2725, 2021.
- [13] H. N. Mohaisen and A. M. Abdalhadi, "Influence of the Induced Magnetic and Rotation on Mixed Convection Heat Transfer for the Peristaltic Transport of Bingham plastic Fluid in an Asymmetric Channel". *Iraqi Journal of Science*, pp. 1770-1785, 2022.
- [14] H. N. Mohaisen and A. M. Abedulhadi, "Effects of the Rotation on the Mixed Convection Heat Transfer Analysis for the Peristaltic Transport of Viscoplastic Fluid in Asymmetric Channel," *Iraqi Journal of Science*, pp. 1240-1257, 2022.